

# Reappraisal of the climate impacts of ozone-depleting substances

Olaf Morgenstern<sup>1,1</sup>, Fiona M. O'Connor<sup>2,2</sup>, Ben T. Thomas Johnson<sup>3,3</sup>, Guang Zeng<sup>4,4</sup>, Jane Patricia Mulcahy<sup>2,2</sup>, Jonny Williams<sup>1,1</sup>, Joao Teixeira<sup>2,2</sup>, Martine Michou<sup>5,5</sup>, Pierre Nabat<sup>6,6</sup>, Larry Wayne Horowitz<sup>7,7</sup>, Vaishali Naik<sup>8,8</sup>, Lori T. Sentman<sup>9,9</sup>, Makoto Deushi<sup>10,10</sup>, Susanne E. Bauer<sup>11,11</sup>, Kostas Tsigaridis<sup>12,12</sup>, Drew T. Shindell<sup>13,13</sup>, and Douglas Edward Kinnison<sup>14,14</sup>

<sup>1</sup>NIWA

<sup>2</sup>Met Office Hadley Centre

<sup>3</sup>UK Met Office

<sup>4</sup>National Institute of Water and Atmospheric Research

<sup>5</sup>Meteo-France

<sup>6</sup>Météo-France

<sup>7</sup>GFDL/NOAA

<sup>8</sup>NOAA GFDL

<sup>9</sup>National Oceanic and Atmospheric Administration/Geophysical Fluid Dynamics Laboratory

<sup>10</sup>Meteorological Research Institute

<sup>11</sup>NASA Goddard Institute for Space Studies, New York, NY, USA

<sup>12</sup>Center for Climate Systems Research, Columbia University, and NASA Goddard Institute for Space Studies

<sup>13</sup>Duke University

<sup>14</sup>NCAR/CLAS

November 30, 2022

## Abstract

We assess the effective radiative forcing due to ozone-depleting substances using models participating in the Aerosols and Chemistry Model Intercomparison Project (AerChemMIP). A large inter-model spread in this globally averaged quantity necessitates an “emergent constraint” approach whereby we link the radiative forcing to the amount of ozone depletion simulated during 1979-2000, excluding two volcanically perturbed periods. During this period ozone-depleting substances were increasing, and several merged satellite-based climatologies document the ensuing decline of total-column ozone. We use these analyses to come up with effective radiative forcing magnitudes. For all of these satellite climatologies we find an effective radiative forcing outside or on the edge of the previously published “likely” range given by the 5th Assessment Report of IPCC, implying an offsetting effect of ozone depletion and/or other atmospheric feedbacks of -0.4 to -0.25 Wm<sup>-2</sup>, which is in absolute terms is larger than the previous best estimate of -0.15 Wm<sup>-2</sup>.

# Reappraisal of the climate impacts of ozone-depleting substances

Olaf Morgenstern<sup>1</sup>, Fiona M. O'Connor<sup>2</sup>, Ben T. Johnson<sup>2</sup>, Guang Zeng<sup>1</sup>, Jane P. Mulcahy<sup>2</sup>, Jonny Williams<sup>1</sup>, João Teixeira<sup>2</sup>, Martine Michou<sup>3</sup>, Pierre Nabat<sup>3</sup>, Larry W. Horowitz<sup>4</sup>, Vaishali Naik<sup>4</sup>, Lori T. Sentman<sup>4</sup>, Makoto Deushi<sup>5</sup>, Susanne E. Bauer<sup>6,7</sup>, Kostas Tsigaridis<sup>7,6</sup>, Drew T. Shindell<sup>8</sup>, Douglas E. Kinnison<sup>9</sup>

<sup>1</sup>National Institute of Water and Atmospheric Research (NIWA), Wellington, New Zealand

<sup>2</sup>Hadley Centre, Met Office, Exeter, UK

<sup>3</sup>Centre National de Recherches Météorologiques (CNRM), Université de Toulouse, Météo-France, CNRS, Toulouse, France

<sup>4</sup>Geophysical Fluid Dynamics Laboratory (GFDL), National Oceanic and Atmospheric Administration, Princeton, NJ, USA

<sup>5</sup>Meteorological Research Institute (MRI), Tsukuba, Japan

<sup>6</sup>NASA Goddard Institute for Space Studies (GISS), New York, NY, USA

<sup>7</sup>Center for Climate Systems Research, Columbia University, New York, NY, USA

<sup>8</sup>Earth & Ocean Sciences, Duke University, Durham, NC, USA

<sup>9</sup>National Center for Atmospheric Research (NCAR), Boulder, CO, USA

## Key Points:

- Effective radiative forcing of ozone-depleting substances, as discerned from CMIP6 models, spans a large range.
- We use an Emergent Constraint technique, relating this effective radiative forcing to ozone changes, to come up with a new range consistent with observational climatologies of ozone depletion.
- This range implies a larger impact of ozone depletion on the effective radiative forcing than the previous best estimate.

---

Corresponding author: Olaf Morgenstern, [olaf.morgenstern@niwa.co.nz](mailto:olaf.morgenstern@niwa.co.nz)

**Abstract**

We assess the effective radiative forcing due to ozone-depleting substances using models participating in the Aerosols and Chemistry Model Intercomparison Project (AerChemMIP). A large inter-model spread in this globally averaged quantity necessitates an “emergent constraint” approach whereby we link the radiative forcing to the amount of ozone depletion simulated during 1979-2000, excluding two volcanically perturbed periods. During this period ozone-depleting substances were increasing, and several merged satellite-based climatologies document the ensuing decline of total-column ozone. We use these analyses to come up with effective radiative forcing magnitudes. For all of these satellite climatologies we find an effective radiative forcing outside or on the edge of the previously published “likely” range given by the 5<sup>th</sup> Assessment Report of IPCC, implying an offsetting effect of ozone depletion and/or other atmospheric feedbacks of  $-0.4$  to  $-0.25$   $\text{Wm}^{-2}$ , which is in absolute terms is larger than the previous best estimate of  $-0.15$   $\text{Wm}^{-2}$ .

**Plain Language Summary**

Chloroflourocarbons and other compounds involved in ozone depletion are also powerful greenhouse gas, but their contribution to global warming is reduced due to the cooling effect of the ozone loss which they induce. Models informing an upcoming climate report disagree on the ozone loss and thus on the climate influence of these gases. Here we use observed ozone loss to reduce the resultant uncertainty in their overall climate influence and infer a larger cooling influence of ozone loss than was previously considered. The result implies a smaller benefit to climate of the phase-out of these ozone-depleting substances, mandated under the Montreal Protocol, than would have been the case under previous understanding.

**1 Introduction**

The Antarctic ozone hole remains arguably the most spectacular demonstration of human interference with the climate system. Within a few decades of starting to use chloro-fluorocarbons (CFCs) and other halocarbons on an industrial scale, humans had thinned the ozone layer above Antarctica in spring to a fraction of its prior thickness (WMO, 2018). This ozone depletion has had a substantial impact on the circulation and climate of the Southern Hemisphere (Velders et al., 2007; Myhre et al., 2013; Shindell et al., 2013). In 1987 the Montreal Protocol was enacted and subsequently strengthened which mandates a phase-out of these ozone-depleting substances (ODSs). It has been hailed as the most successful international treaty ever to protect the environment. Several of these ODSs also act as greenhouse gases, with global warming potentials many 1000’s of times larger than that of carbon dioxide (WMO, 2018). By phasing them out, it is thought that the Montreal Protocol has averted more global warming than the Kyoto Protocol (Velders et al., 2007) despite not being designed for this purpose. The 5<sup>th</sup> Assessment Report of IPCC (AR5, Myhre et al., 2013) estimates that in 2011 the ODSs regulated by the Montreal Protocol exerted a direct radiative forcing of  $0.34$   $\text{Wm}^{-2}$  and an indirect radiative forcing due to ozone depletion of  $-0.15 \pm 0.15$   $\text{Wm}^{-2}$  relative to pre-industrial times. Accordingly, AR5 assesses that ODSs “very likely” have a positive radiative forcing as their direct radiative effects outweigh the indirect impact of ozone depletion.

The AR5 assessment was based essentially on one model (Shindell et al., 2013); also there is a large uncertainty associated with the negative radiative forcing due to ozone depletion. Furthermore, AR5 used the “stratospherically adjusted radiative forcing” concept, whereby any atmospheric adjustments other than a temperature adjustment of the stratosphere are not considered. AR5 stipulated that the effects of these were minor. These issues motivate a reassessment using new models and more developed methodologies. AerChemMIP (a subsidiary of the 6<sup>th</sup> Coupled Model Intercomparison Project, CMIP6; Collins et al., 2017) is a coordinated effort to re-assess these radiative forcing processes using

77 newer models and taking into account all atmospheric adjustments, arriving at the “ef-  
 78 fective radiative forcing” (ERF, Forster et al., 2016). In particular, here we will use sim-  
 79 ulations submitted under the “piClim-control” and the “piClim-HC” experiments. Both  
 80 are atmosphere-only simulations driven with preindustrial sea-surface conditions and all  
 81 atmospheric forcings at preindustrial levels, except that in the case of piClim-HC sur-  
 82 face abundances of halogenated ODSs (short: halocarbons, HCs) compounds are elevated  
 83 to their 2014 mean surface volume mixing ratios (Meinshausen et al., 2017). The differ-  
 84 ence in the global, multi-annual mean net top-of-the-atmosphere radiation between this  
 85 pair of simulations defines the ERF due to ODSs. The problem, detailed below, is that  
 86 this approach yields large inter-model differences for this ERF. This is a familiar situ-  
 87 ation in climate modelling. The “equilibrium climate sensitivity” (ECS, the equilibrium  
 88 warming of the planet for a doubling of CO<sub>2</sub>) is another well-studied example of sim-  
 89 ilarly large inter-model spread (for a recent discussion see Zelinka et al., 2020). A tech-  
 90 nique to deal with such model disparities is known as an “emergent constraint” (e.g., Williamson  
 91 & Sansom, 2019). This consists of relating a theoretical concept (such as the ECS or the  
 92 ERF of ODSs, the topic of this paper) to a different, physically related quantity for which  
 93 good-quality historical observational data exist. To constrain the ERF of ODSs, we eval-  
 94 uate here the choice of total-column ozone (TCO) measured comprehensively by satel-  
 95 lite and ground-based instruments since the latter decades of the 20<sup>th</sup> century when ODSs  
 96 were sharply increasing over time and ozone depletion was established. The remainder  
 97 of this paper is devoted to applying this approach to AerChemMIP and “historical” (Eyring  
 98 et al., 2016) simulations to arrive at a recommended value for the ERF of ODSs.

## 99 2 Models

100 We use here six different climate models, listed in table 1. The two GISS models  
 101 differ in their coupled ocean models but have identical atmosphere and other sub-models.

Model name	Reference	Historical simulations
CESM2-WACCM	Gettelman et al. (2019)	1, 2, 3
CNRM-ESM2-1	S��f��rian et al. (2019)	1 to 5, 8, 9, 10
GFDL-ESM4	Dunne and et al. (2020)	1
GISS-E2-1-G/H	Kelley et al. (2019)	6, 8, 9, 10
MRI-ESM2-0	Yukimoto et al. (2019)	1 to 5
UKESM1-0-LL	Sellar et al. (2019)	1 to 4, 8 to 12, 16 to 19

**Table 1.** Models, key references, and “historical” simulations denoted by their run numbers.

102 The models are chosen because (a) all of them have explicit stratospheric chem-  
 103 istry, and (b) required data from these models is available for the piClim-control, piClim-  
 104 HC, and historical experiments. Here we use total-column (or vertically resolved ozone,  
 105 in the case of CESM2-WACCM) and outgoing short- and longwave radiation at the top  
 106 of the atmosphere, all in monthly-means. The piClim-control and piClim-HC experiments  
 107 all are one-member ensembles; the last 20 years of these simulations are used. We have  
 108 established that the halocarbon increase in the piClim-HC simulation versus piClim-control  
 109 has been fully communicated to the ozone layer and the ensuing ozone depletion is fully  
 110 realized (figure S1).

111 In addition to these model data, we use five different ozone climatologies listed in  
 112 table 2. Here we only consider data from the period 1979-2000 when ozone depletion was  
 113 established. Four of these datasets are based on satellite measurements (instruments such  
 114 as the Solar Backscatter Ultraviolet Radiometer (SBUV) series are used in all of them)  
 115 but may use different versions and/or combine them in different ways with ground-based  
 116 measurements to account for offsets between different overlapping satellite timeseries,

117 data gaps, drifts, and other instrumental artefacts. Details are in the references given  
 118 (table 2). Furthermore, for reference we also consider total-column ozone derived from  
 119 the recommended CMIP6 ozone forcing dataset (Checa-Garcia et al., 2018) used by CMIP6  
 120 models that do not compute their own ozone (i.e. not the six models listed in table 1).  
 121 Referred to here as “CMIP6”, this is not an observational dataset; rather it is derived  
 122 from two historical chemistry-climate model simulations including one by CESM1-WACCM,  
 123 an older version of the CESM2-WACCM model figuring in this study. In all references  
 124 and in the “historical” simulations we remove two years each after the major eruptions  
 125 of El Chichón (March 1982) and Mt Pinatubo (June 1991) although retaining these data  
 126 would only have a small influence on our results.

Dataset	Coverage	Resolution	Reference
TOMS-SBUV v8	1978-2005	Zonal-mean, 5°	Frith et al. (2014)
SBUV v8.6	1970-2018	Zonal mean, 5°	Frith et al. (2014)
NIWA-BS (v3.4, unpatched)	1978-2016	1° × 1°	Bodeker et al. (2005)
MSR-2	1979-2018	0.5° × 0.5°	van der A et al. (2015)
CMIP6	1850-2014	2.5° × 1.5°	Checa-Garcia et al. (2018)

**Table 2.** Four observational TCO climatologies and the reference ozone field used to force CMIP6 models without interactive ozone.

### 127 3 Results

128 We calculate trends in TCO for the period 1979-2000 for the five reference dataset  
 129 and the six models (figure 1) excluding two years each after the El Chichón and Mt Pinatubo  
 130 eruptions in 1982 and 1991. There are mostly relatively small differences between the  
 131 observational datasets, as expected. The Multi-Sensor Reanalysis 2 (MSR-2) dataset uses  
 132 data assimilation in a chemistry-transport model (van der A et al., 2015). As such it has  
 133 a more comprehensive coverage than the other climatologies. It reveals substantial ozone  
 134 loss in the Arctic peaking in March when the other three observational datasets have data  
 135 gaps. It has slightly weaker Antarctic ozone depletion than the NIWA-Bodeker Scien-  
 136 tific (NIWA-BS), SBUV, and TOMS-SBUV climatologies. MSR-2 has the winter polar  
 137 observational gaps characteristic of satellite measurements largely or completely filled  
 138 in (in the case of the Arctic), in contrast to NIWA-BS, SBUV, and TOMS-SBUV. The  
 139 SBUV climatology does not have any data poleward of 80°N/S, i.e. it has the most re-  
 140 stricted high-latitude coverage of the datasets considered here. TOMS-SBUV is very sim-  
 141 ilar to the SBUV dataset but in summer does not have data gaps over both polar caps.

142 The CMIP6 ozone climatology compares well with the observations in the South-  
 143 ern Hemisphere but underestimates the decline in Northern-Hemisphere ozone. This is  
 144 most evident in comparison to MSR-2 but can also be seen versus the other three datasets.

145 The six climate models exhibit highly variable Antarctic ozone trends in their ensemble-  
 146 average historical simulations (figure 1), ranging from quite weak (MRI-ESM2-0) to ex-  
 147 tremely strong (GISS-E2-1-G and GISS-E2-1-H). Also in the Arctic, several models ex-  
 148 hibit weak trends, with the exception of UKESM1 which exhibits excessive ozone deple-  
 149 tion in both polar regions.

150 We next address the extent to which these historical ozone trends represent ozone  
 151 loss attributable to ODSs. Considerations here include that at least in models, and likely  
 152 in reality, some reductions in stratospheric ozone occurred before the onset of compre-  
 153 hensive satellite measurements in 1978 (figure S2, Dhomse et al., 2018), that the actual  
 154 ozone depletion occurred in an atmosphere with the methane loading increased above

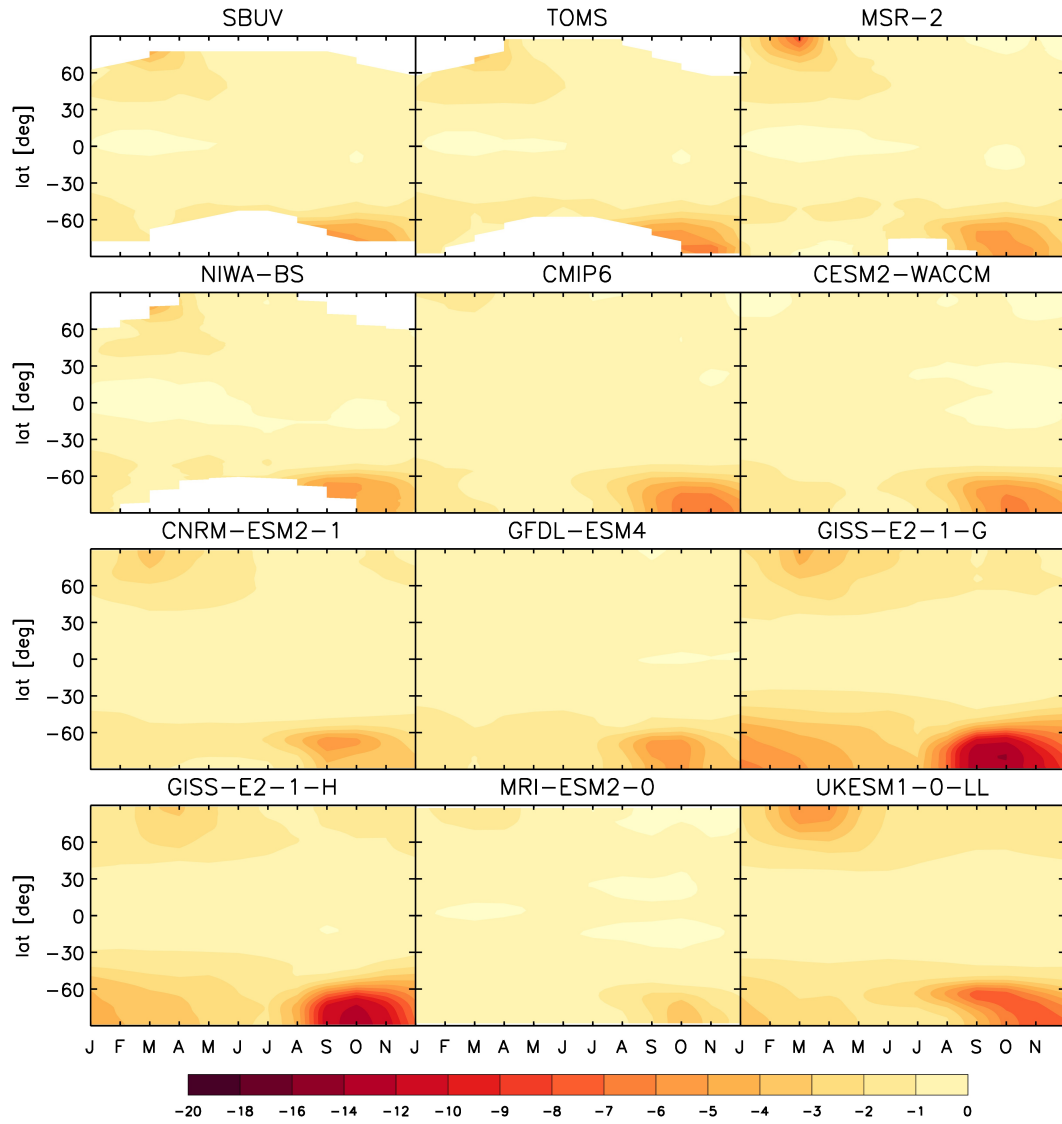


**Figure 1.** Zonal-mean TCO trends (Dobson Unit/year,  $\text{DU a}^{-1}$ ) for 1979-2000, excluding two years each after the El Chichón and Pinatubo eruptions, in four observational datasets (SBUV, TOMS-SBUV, NIWA-BS, and MSR-2), the CMIP6 ozone climatology, and the historical simulations by the seven CMIP6 models considered here.

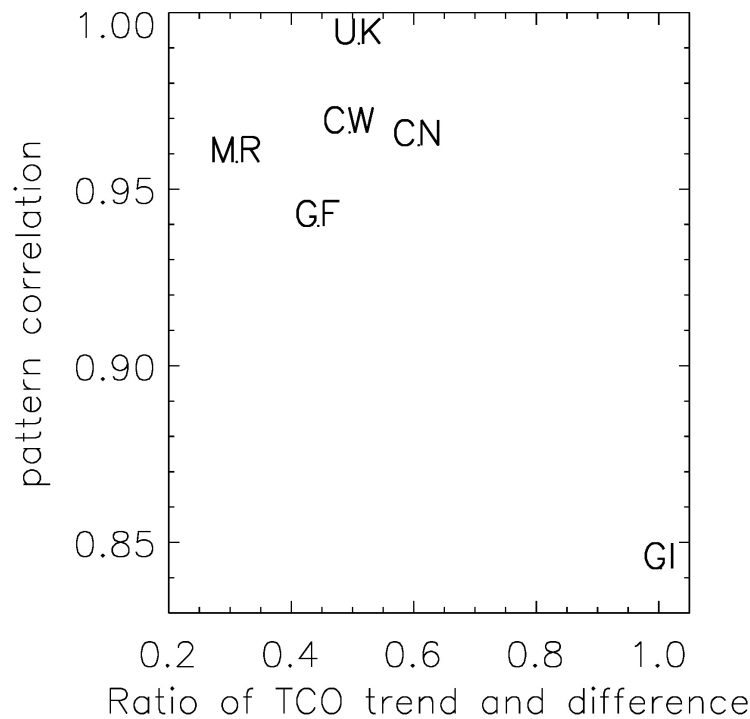


**Figure 2.** Abscissa: Ratio of area-weighted, global- and annual-mean ozone trend ( $\text{DU a}^{-1}$ ) for 1979-2000 derived from the historical simulations, with two volcanically perturbed periods removed (figure 1) and the global- and annual-mean mean ozone difference (DU) between the piClim-HC and piClim-control experiments (figure S1) divided by 22 years. Ordinate: Pattern correlation between the zonal-mean ozone trends shown in figure 1 and the zonal-mean ozone differences between the piClim-HC and piClim-control experiments, for the six CMIP6 models. CN = CNRM-ESM2-1. CW- CESM2-WACCM. GF = GFDL-ESM4. GI = GISS-E2-1-G. MR = MRI-ESM2-0. UK = UKESM1-0-LL.

155 its preindustrial level which reduces the efficiency of chlorine at depleting ozone, and that  
156 stratospheric cooling since preindustrial times due to increasing greenhouse gases (GHGs)  
157 affects both polar and extrapolar ozone chemistry in different ways (Morgenstern et al.,  
158 2018). Single-forcing model simulations consistently show that the net effect of these GHGs  
159 increasing during the ozone-depletion period has been to mitigate some ozone depletion  
160 (Eyring et al., 2010; Dhomse et al., 2018). Figure S3 shows the difference of zonal-mean  
161 ozone between the piClim-control and piClim-HC experiments for the six models. A vi-  
162 sual comparison to figure 1 indicates a high degree of pattern similarity for most mod-  
163 els between the late-20<sup>th</sup> century ozone trends shown in figure 1 and the ozone loss at-  
164 tributable to ODSs. An exception to this is the GISS-E2-1-G model which has an anoma-  
165 lously large Southern-Hemisphere ozone trend associated with the formation of the ozone  
166 hole, but an ozone difference in figure S3 that is not anomalous relative to the other mod-  
167 els.

168 Figure 2 displays a measure of the similarity between figures 1 and S3 for the six  
169 models. Five models cluster at a pattern correlation exceeding 0.94 and a trend to dif-  
170 ference ratio of around 0.3 to 0.6 (i.e. the global ozone loss deduced from historical sim-  
171 ulations between 1979 and 2000 is 30 to 60% of the difference in ozone between the piClim-  
172 control and piClim-HC simulations). GISS-E2-1-G has a somewhat lower correlation but  
173 a much larger trend ratio. Figure S2 shows that this model exhibits a much bigger re-  
174 sponse to volcanic eruptions than the other models (e.g. after the Krakatoa eruption of  
175 1883) and enters into a volcanically disturbed phase of increased TCO in the 1970s. This  
176 implies that in this model, the 1979-2000 trend has a substantial contribution due to re-  
177 covery from this volcanic perturbation. This manifests as an anomalous amplification  
178 of the influence of ODSs as the volcanic effect transitions from increasing TCO under  
179 low chlorine conditions to decreasing it during times of high chlorine loading. For this  
180 reason GISS-E2-1-G is not considered in the further analysis.

181 Figure 3 illustrates the “emergent constraint” relating simulated mean TCO loss  
182 for 1979-2000 (excluding volcanic periods) to the mean ERF of ODSs discerned from the  
183 piClim-control and piClim-HC experiments. The figure shows that this ERF closely re-  
184 lates to how much ozone depletion is simulated in these models. We capture this rela-  
185 tionship through a least-squares linear regression line. Where this line intersects with  
186 the ozone depletion discerned from an observational climatology defines the ERF of ODSs  
187 that optimally corresponds to the ozone loss in that climatology. This process is illus-  
188 trated in figure 3 for the example of the NIWA-BS climatology (similar plots for the other  
189 climatologies are in the supplement, figures S4 to S7). Here sampling the modeled TCO  
190 data in the same way as this climatology makes the modelled and observational clima-  
191 tologies directly comparable. Table 3 summarizes the ERFs discerned in this way using  
192 all TCO climatologies considered here as well as their means and standard deviations.  
193 A comparison with the straightforward multi-model mean (MMM) using the six mod-  
194 els considered here (table 3) reveals that the multi-model mean is often outside the one-  
195 standard deviation uncertainty range spanned by the Emergent Constraint analyses, and  
196 that these analyses lead a considerably reduction of the uncertainty relative to forming  
197 the multi-model mean. A caveat in both cases is that the uncertainty analysis presented  
198 here does not capture some aspects of the total uncertainty such as sampling uncertainty  
199 (caused by the small number of models considered here) and model uncertainty (caused  
200 by structural and formulation problems inherent in models, which may be common to  
201 different models).

## 202 4 Discussion

203 Our analysis has shown that historical TCO trends for 1979-2000 simulated by CMIP6  
204 full-chemistry models, with volcanic periods ignored, can serve as proxies for the total  
205 ozone loss caused by anthropogenic ODSs simulated by the same models. This enables  
206 us to conduct an “emergent constraint” analysis, relating this historical ozone loss to the

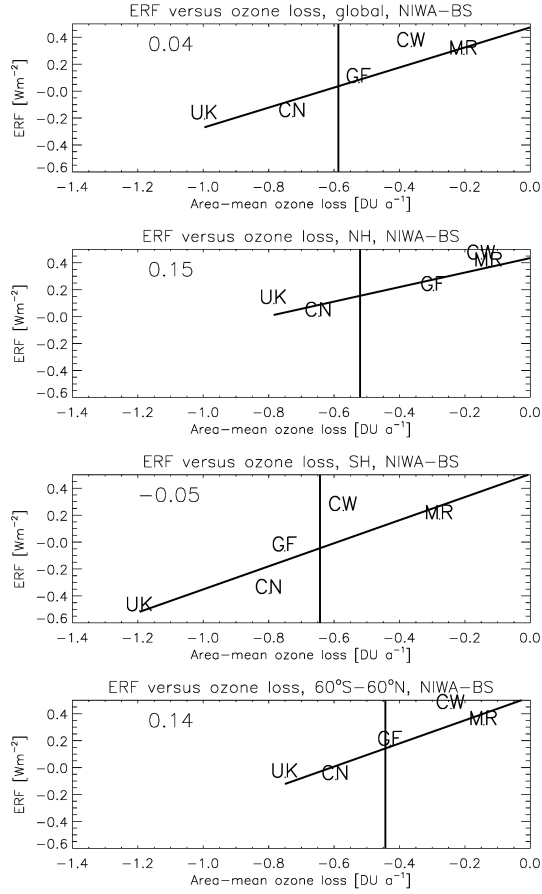


**Figure 3.** Abscissa: Area-weighted global- and annual-mean ozone loss (DU a<sup>-1</sup>) for 1979-2000, discerned from the historical simulations of five CMIP6 models. Vertical line: Same, for the NIWA-Bodeker Scientific climatology. Ordinate: The ERF of ODSs as discerned from the piClim-HC and piClim-control simulations of these five models. Slanted line: linear regression. The four panels denote global, Southern-Hemisphere, Northern-Hemisphere, and 60°S to 60°N averages. The numbers inside the plots are the ERF values corresponding to the ozone loss discerned from the NIWA-BS climatology. CN = CNRM-ESM2-1. CW- CESM2-WACCM. GF = GFDL-ESM4. MR = MRI-ESM2-0. UK = UKESM1-0-LL. Equivalent plots for the other climatologies are in the supplement.

Climatology	90°S-90°N	0°-90°N	90°S-0°	60°S-60°N
CESM2-WACCM	0.31	0.43	0.19	0.41
CNRM-ESM2-1	-0.19	0.00	-0.38	-0.09
GFDL-ESM4	0.06	0.19	-0.07	0.16
GISS-E2-1-G	0.28	0.23	0.33	0.38
MRI-ESM2-0	0.30	0.40	0.20	0.34
UKESM1-0-LL	-0.19	0.12	-0.50	-0.06
MMM $\pm\sigma$	0.10 $\pm$ 0.25	0.23 $\pm$ 0.16	-0.04 $\pm$ 0.34	0.19 $\pm$ 0.22
MSR-2	0.09	0.20	0.01	0.18
NIWA-BS	0.04	0.15	-0.05	0.14
SBUV	0.00	0.15	-0.12	0.09
TOMS-SBUV	-0.06	0.12	-0.20	0.03
MOM $\pm\sigma$	0.02 $\pm$ 0.06	0.16 $\pm$ 0.03	-0.09 $\pm$ 0.09	0.11 $\pm$ 0.06
CMIP6	0.13	0.32	-0.09	0.23

**Table 3.** ERFs of ODSs ( $\text{Wm}^{-2}$ ). Top seven rows: Model results and multi-model mean (MMM) and standard deviation ( $\sigma$ ). Bottom five rows: Results of the "emergent constraint" analysis and its mean ("multi-observations mean", MOM) and standard deviation.

207 ERF of ODSs simulated in five CMIP6 models. We find that indeed the ozone loss cor-  
 208 relates with the ERF of ODSs, and that observed TCO loss provides the "emergent con-  
 209 straint" on an otherwise highly uncertain quantity. This analysis depends to some ex-  
 210 tent on the ozone depletion evident in the observational climatologies. The differences  
 211 between them are small; they differ in their coverage of high-latitude and polar-night sit-  
 212 uations. However even if the analysis is restricted to extrapolar latitudes, removing the  
 213 influence of such artefacts, some differences remain. Relative to the four observational  
 214 climatologies, the ERF of ODSs falls into the range of  $-0.06$  to  $+0.09 \text{ Wm}^{-2}$ . Assum-  
 215 ing now that the direct radiative forcing due to ODSs is  $0.34 \text{ Wm}^{-2}$  (Myhre et al., 2013),  
 216 that means all other feedbacks (associated with ozone depletion, but also cloud and aerosol  
 217 responses) cause an effective radiative forcing in the range of  $-0.4$  to  $-0.25 \text{ Wm}^{-2}$ . (As  
 218 an aside, the CFC-12 equivalent mixing ratio of ODSs only dropped by 0.4% between  
 219 2011 and 2014; Meinshausen et al., 2017, meaning this direct radiative forcing is essen-  
 220 tially unchanged during this period.)

221 Extrapolation of the regression line in figure 3 to zero ozone loss yields a global-  
 222 mean ERF of ODSs, thus excluding the direct and indirect impacts of ozone depletion,  
 223 of  $0.45$  to  $0.55 \text{ Wm}^{-2}$  in all cases. This is slightly larger than the AR5 estimate for the  
 224 direct radiative forcing of ODSs of  $0.34 \text{ Wm}^{-2}$  (Myhre et al., 2013), possibly because of  
 225 additional feedbacks not included in the AR5 calculation, but also possibly highlight-  
 226 ing that the "emergent constraint" analysis conducted here is based on only five mod-  
 227 els all using low spectral-resolution radiative transfer schemes, and hence is somewhat  
 228 uncertain. (The uncertainty range stated above only includes the part of the uncertainty  
 229 stemming from the different observational ozone climatologies, not any other, model-related  
 230 uncertainty.)

231 For all ozone climatologies, the analysis suggests a near-zero or negative total ERF  
 232 of ODSs in the Southern Hemisphere of between  $+0.01$  and  $-0.20 \text{ Wm}^{-2}$  (table 3), im-  
 233 plying a cooling effect of ozone depletion and other feedback processes of between  $-0.33$   
 234 and  $-0.54 \text{ Wm}^{-2}$  (again based on the AR5 globally averaged direct radiative forcing es-  
 235 timate of  $0.34 \text{ Wm}^{-2}$  which we assume is also the Southern-Hemisphere average). For  
 236 the Northern Hemisphere, in all cases the analysis yields positive ERFs, reflecting the

237 lesser role of ozone depletion here. If the analysis is restricted to the latitude range  $60^{\circ}\text{S}$   
238 to  $60^{\circ}\text{N}$ , thus excluding the polar regions affected by variably large data gaps, the range  
239 of values (maximum – minimum) is the same ( $0.15 \text{ Wm}^{-2}$ ) as if the analysis is extended  
240 to all grid points with valid data in the observational references, suggesting that the mid-  
241 and low-latitude differences between the TCO climatologies play a significant role in driv-  
242 ing the uncertainty in the global ERF.

243 Turning now to the CMIP6 ozone climatology (Checa-Garcia et al., 2018), the weak  
244 Northern-Hemisphere ozone depletion in this climatology, relative to observations, causes  
245 a smaller absolute ERF of ozone changes and hence a larger total global-mean ERF ( $0.13$   
246  $\text{Wm}^{-2}$ ) than would be consistent with the observations. In the Southern Hemisphere,  
247 ozone loss and thus the ERF of ODSs associated with this climatology ( $-0.09 \text{ Wm}^{-2}$ )  
248 compare well with the observational estimates. The ERF associated with this climatol-  
249 ogy, for all four latitude regions, is close to but consistently smaller than the ERFs cal-  
250 culated for the CESM2-WACCM model (table 3). This behavior, paralleling CESM2-  
251 WACCM, is as expected as this model, in an older version, was one of two models used  
252 in the generation of the climatology (Checa-Garcia et al., 2018).

253 In summary, we find here a global-mean offsetting effect of ozone depletion on the  
254 ERF of ODSs which is only marginally overlapping the “likely” range given in AR5 of  
255  $-0.3$  to  $0 \text{ Wm}^{-2}$ . The best estimate of AR5,  $-0.15 \text{ Wm}^{-2}$ , is outside the range derived  
256 here. Reasons for this difference may include (a) conceptual differences between the “strato-  
257 spherically adjusted radiative forcing” evaluated in AR5 and the ERF evaluated here;  
258 (b) model differences, whereby the AR5 estimate was based on one model only (Shindell  
259 et al., 2013) – our analysis reveals a large model dependence of the result; and (c) method-  
260 ological differences, whereby here we account for observational references using an novel  
261 “emergent constraint” approach. This approach turns large inter-model differences from  
262 a problem into an asset necessary for the regression analysis to become robust. A down-  
263 side of the approach is that influences other than ODSs (such as increasing GHGs, tropo-  
264 spheric ozone pollution, or variations in solar output) have not been explicitly accounted  
265 for in the observational record (we have removed some volcanically affected periods), so  
266 there may be scope to further refine this analysis. In a follow-on publication we will en-  
267 deavour to shed more light on the role of secondary feedbacks which in combination make  
268 up “effective radiative forcing” (namely chemical ozone depletion, cloud and tempera-  
269 ture adjustments, and aerosol feedbacks). This analysis cannot be conducted based only  
270 on AerChemMIP simulations and hence is beyond the scope of this paper.

## 271 Acknowledgments

272 OM, FOC, BJ, GZ, JPM, JW, and JT acknowledge the UKESM1 team and other col-  
273 leagues for their support, in particular, Luke Abraham, Paul Griffiths, Mohit Dalvi, James  
274 Manners, and Omar Jamil. OM and GZ were supported by the NZ Government’s Strate-  
275 gic Science Investment Fund (SSIF) through the NIWA programme CACV. FOC, BJ,  
276 and JPM were supported by the Met Office Hadley Centre Climate Programme funded  
277 by BEIS and Defra (Grant Number GA01101). JW acknowledges support by the Deep  
278 South National Science Challenge (DSNSC), funded by the New Zealand Ministry for  
279 Business, Innovation and Employment (MBIE). The authors acknowledge the contribu-  
280 tion of NeSI high-performance computing facilities to the results of this research. New  
281 Zealand’s national facilities are provided by the New Zealand eScience Infrastructure (NeSI)  
282 and funded jointly by NeSI’s collaborator institutions and through MBIE’s Research In-  
283 frastructure programme. MM and PN particularly acknowledge the support of the en-  
284 tire team in charge of the CNRM climate models, and especially that of Antoinette Alias  
285 and Laurent Franchisteguy for their technical assistance. Supercomputing time was pro-  
286 vided by the Météo-France/DSI supercomputing center. Makoto Deushi was partly sup-  
287 ported by JSPS KAKENHI grant no. JP20K04070. The CESM project is supported pri-  
288 marily by the National Science Foundation (NSF). This material is based upon work sup-

ported by the National Center for Atmospheric Research (NCAR), which is a major facility sponsored by the NSF under Cooperative Agreement 1852977. Computing and data storage resources, including the Cheyenne supercomputer (doi:10.5065/D6RX99HX), were provided by the Computational and Information Systems Laboratory (CISL) at NCAR.

We thank Bodeker Scientific, funded by the DSNSC, NASA, and KNMI for providing the total-column ozone databases. Data used in this study are all publicly available at [https://acd-ext.gsfc.nasa.gov/Data\\_services/merged/data/additional\\_files/toms\\_sbuvs.v8.mod.v3.78-05.za.rev2.txt](https://acd-ext.gsfc.nasa.gov/Data_services/merged/data/additional_files/toms_sbuvs.v8.mod.v3.78-05.za.rev2.txt), [https://acd-ext.gsfc.nasa.gov/Data\\_services/merged/data/sbuvs.v86.mod.int\\_lyr.70-18.za.r7.txt](https://acd-ext.gsfc.nasa.gov/Data_services/merged/data/sbuvs.v86.mod.int_lyr.70-18.za.r7.txt), <http://www.bodekerscientific.com/data/total-column-ozone>, <http://www.temis.nl/protocols/O3global.html>, and the CMIP6 portals (<https://esgf-node.llnl.gov/search/cmip6/> and <https://esgf-node.llnl.gov/search/input4mips/>).

## References

- Bodeker, G. E., Shiona, H., & Eskes, H. (2005). Indicators of Antarctic ozone depletion. *Atmospheric Chemistry and Physics*, *5*, 2603–2615. doi: 10.5194/acp-5-2603-2005
- Checa-Garcia, R., Hegglin, M. I., Kinnison, D., Plummer, D. A., & Shine, K. P. (2018). Historical tropospheric and stratospheric ozone radiative forcing using the CMIP6 database. *Geophysical Research Letters*, *45*(7), 3264–3273. Retrieved from <https://agupubs.onlinelibrary.wiley.com/doi/abs/10.1002/2017GL076770> doi: 10.1002/2017GL076770
- Collins, W. J., Lamarque, J.-F., Schulz, M., Boucher, O., Eyring, V., Hegglin, M. I., ... Smith, S. J. (2017). AerChemMIP: Quantifying the effects of chemistry and aerosols in CMIP6. *Geoscientific Model Development*, *10*(2), 585–607. Retrieved from <https://www.geosci-model-dev.net/10/585/2017/> doi: 10.5194/gmd-10-585-2017
- Dhomse, S. S., Kinnison, D., Chipperfield, M. P., Salawitch, R. J., Cionni, I., Hegglin, M. I., ... Zeng, G. (2018). Estimates of ozone return dates from Chemistry-Climate Model Initiative simulations. *Atmospheric Chemistry and Physics*, *18*, 8409–8438.
- Dunne, J. P., & et al. (2020). The GFDL Earth System Model version 4.1 (GFDL-ESM4.1): Model description and simulation characteristics. *in prep.*
- Eyring, V., Bony, S., Meehl, G. A., Senior, C. A., Stevens, B., Stouffer, R. J., & Taylor, K. E. (2016). Overview of the Coupled Model Intercomparison Project Phase 6 (CMIP6) experimental design and organization. *Geoscientific Model Development*, *9*(5), 1937–1958. Retrieved from <https://www.geosci-model-dev.net/9/1937/2016/> doi: 10.5194/gmd-9-1937-2016
- Eyring, V., Cionni, I., Bodeker, G. E., Charlton-Perez, A. J., Kinnison, D. E., Scinocca, J. F., ... Yamashita, Y. (2010). Multi-model assessment of stratospheric ozone return dates and ozone recovery in CCMVal-2 models. *Atmospheric Chemistry Physics*, *10*, 9451–9472. Retrieved from <https://doi.org/10.5194/acp-10-9451-2010>
- Forster, P. M., Richardson, T., Maycock, A. C., Smith, C. J., Samset, B. H., Myhre, G., ... Schulz, M. (2016). Recommendations for diagnosing effective radiative forcing from climate models for cmip6. *Journal of Geophysical Research: Atmospheres*, *121*(20), 12,460–12,475. Retrieved from <https://agupubs.onlinelibrary.wiley.com/doi/abs/10.1002/2016JD025320> doi: 10.1002/2016JD025320
- Frith, S. M., Kramarova, N. A., Stolarski, R. S., McPeters, R. D., Bhartia, P. K., & Labow, G. J. (2014). Recent changes in total column ozone based on the SBUV version 8.6 merged ozone data set. *Journal of Geophysical Research: Atmospheres*, *119*(16), 9735–9751. Retrieved from <https://>

- 341 agupubs.onlinelibrary.wiley.com/doi/abs/10.1002/2014JD021889 doi:  
342 10.1002/2014JD021889
- 343 Gettelman, A., Mills, M. J., Kinnison, D. E., Garcia, R. R., Smith, A. K., Marsh,  
344 D. R., ... Randel, W. J. (2019). The Whole Atmosphere Commu-  
345 nity Climate Model version 6 (WACCM6). *Journal of Geophysical Re-*  
346 *search: Atmospheres*, 124(23), 12380-12403. Retrieved from [https://](https://agupubs.onlinelibrary.wiley.com/doi/abs/10.1029/2019JD030943)  
347 [agupubs.onlinelibrary.wiley.com/doi/abs/10.1029/2019JD030943](https://agupubs.onlinelibrary.wiley.com/doi/abs/10.1029/2019JD030943) doi:  
348 10.1029/2019JD030943
- 349 Kelley, M., Schmidt, G. A., Nazarenko, L., Miller, R. L., Bauer, S. E., Ruedy, R.,  
350 ... Yao, M. (2019). GISS-E2.1: Configurations and climatology. *Journal of*  
351 *Advances in Modelling Earth Systems*. (Manuscript submitted for publication)
- 352 Meinshausen, M., Vogel, E., Nauels, A., Lorbacher, K., Meinshausen, N., Etheridge,  
353 D. M., ... Weiss, R. (2017). Historical greenhouse gas concentrations for  
354 climate modelling (CMIP6). *Geoscientific Model Development*, 10, 2057–2116.  
355 Retrieved from <https://doi.org/10.5194/gmd-10-2057-2017>
- 356 Morgenstern, O., Stone, K. A., Schofield, R., Akiyoshi, H., Yamashita, Y., Kinnison,  
357 D. E., ... Chipperfield, M. P. (2018). Ozone sensitivity to varying green-  
358 house gases and ozone-depleting substances in CCM1-1 simulations. *Atmos.*  
359 *Chem. Phys.*, 18, 1091–1114. Retrieved from [https://doi.org/10.5194/](https://doi.org/10.5194/acp-18-1091-2018)  
360 [acp-18-1091-2018](https://doi.org/10.5194/acp-18-1091-2018)
- 361 Myhre, G., Shindell, D., Bréon, F.-M., Collins, W., Fuglestedt, J., Huang, J., ...  
362 Zhang, H. (2013). Anthropogenic and Natural Radiative Forcing. In *Climate*  
363 *Change 2013 - The Physical Science Basis* (chap. 8). Geneva, Switzerland:  
364 Intergovernmental Panel on Climate Change (IPCC).
- 365 Sellar, A. A., Jones, C. G., Mulcahy, J. P., Tang, Y., Yool, A., Wiltshire, A., ...  
366 Zerroukat, M. (2019). UKESM1: Description and evaluation of the U.K. Earth  
367 System Model. *Journal of Advances in Modeling Earth Systems*, 11(12), 4513-  
368 4558. Retrieved from [https://agupubs.onlinelibrary.wiley.com/doi/abs/](https://agupubs.onlinelibrary.wiley.com/doi/abs/10.1029/2019MS001739)  
369 [10.1029/2019MS001739](https://agupubs.onlinelibrary.wiley.com/doi/abs/10.1029/2019MS001739) doi: 10.1029/2019MS001739
- 370 Shindell, D., Faluvegi, G., Nazarenko, L., Bowman, K., Lamarque, J.-F., Voulgar-  
371 akis, A., ... Ruedy, R. (2013). Attribution of historical ozone forcing to  
372 anthropogenic emissions. *Nature Climate Change*, 3, 567.
- 373 Séférian, R., Nabat, P., Michou, M., Saint-Martin, D., Voltaire, A., Colin, J., ...  
374 Madec, G. (2019). Evaluation of CNRM Earth System Model, CNRM-ESM2-  
375 1: Role of earth system processes in present-day and future climate. *Jour-*  
376 *nal of Advances in Modeling Earth Systems*, 11(12), 4182-4227. Retrieved  
377 from [https://agupubs.onlinelibrary.wiley.com/doi/abs/10.1029/](https://agupubs.onlinelibrary.wiley.com/doi/abs/10.1029/2019MS001791)  
378 [2019MS001791](https://agupubs.onlinelibrary.wiley.com/doi/abs/10.1029/2019MS001791) doi: 10.1029/2019MS001791
- 379 van der A, R. J., Allaart, M. A. F., & Eskes, H. J. (2015). Extended and refined  
380 multi sensor reanalysis of total ozone for the period 1970–2012. *Atmospheric*  
381 *Measurement Techniques*, 8, 3021–3035. Retrieved from [https://doi.org/10](https://doi.org/10.5194/amt-8-3021-2015)  
382 [.5194/amt-8-3021-2015](https://doi.org/10.5194/amt-8-3021-2015)
- 383 Velders, G. J. M., Andersen, S. O., Daniel, J. S., Fahey, D. W., & McFarland, M.  
384 (2007). The importance of the Montreal Protocol in protecting climate. *Pro-*  
385 *ceedings of the National Academy of Sciences*, 104, 4814-4819.
- 386 Williamson, D. B., & Sansom, P. G. (2019). How are emergent constraints quantify-  
387 ing uncertainty and what do they leave behind? *Bulletin of the American Me-*  
388 *teorological Society*, 100(12), 2571-2588. Retrieved from [https://doi.org/10](https://doi.org/10.1175/BAMS-D-19-0131.1)  
389 [.1175/BAMS-D-19-0131.1](https://doi.org/10.1175/BAMS-D-19-0131.1) doi: 10.1175/BAMS-D-19-0131.1
- 390 WMO. (2018). *Scientific Assessment of Ozone Depletion: 2018*. Geneva, Switzer-  
391 land: World Meteorological Organization.
- 392 Yukimoto, S., Kawai, H., Koshiro, T., Oshima, N., Yoshida, K., Urakawa, S., ...  
393 ISHII, M. (2019). The Meteorological Research Institute Earth System Model  
394 Version 2.0, MRI-ESM2.0: Description and basic evaluation of the physical  
395 component. *Journal of the Meteorological Society of Japan Ser. II, advpub.*

396 doi: 10.2151/jmsj.2019-051  
397 Zelinka, M. D., Myers, T. A., McCoy, D. T., Po-Chedley, S., Caldwell, P. M.,  
398 Ceppi, P., . . . Taylor, K. E. (2020). Causes of higher climate sensitivity  
399 in CMIP6 models. *Geophysical Research Letters*, 47(1), e2019GL085782.  
400 Retrieved from [https://agupubs.onlinelibrary.wiley.com/doi/abs/](https://agupubs.onlinelibrary.wiley.com/doi/abs/10.1029/2019GL085782)  
401 10.1029/2019GL085782 (e2019GL085782 10.1029/2019GL085782) doi:  
402 10.1029/2019GL085782